



OPEN

Isolation and characterisation of novel phages infecting *Lactobacillus plantarum* and proposal of a new genus, “Silenusvirus”

Ifigenia Kyrkou^{1,2}, Alexander Byth Carstens^{1,3}, Lea Ellegaard-Jensen¹, Witold Kot^{1,3}, Athanasios Zervas¹, Amaru Miranda Djurhuus^{1,3}, Horst Neve⁴, Charles M. A. P. Franz⁴, Martin Hansen¹ & Lars Hestbjerg Hansen^{1,3}✉

Bacteria of *Lactobacillus* sp. are very useful to humans. However, the biology and genomic diversity of their (bacterio)phage enemies remains understudied. Knowledge on *Lactobacillus* phage diversity should broaden to develop efficient phage control strategies. To this end, organic waste samples were screened for phages against two wine-related *Lactobacillus plantarum* strains. Isolates were shotgun sequenced and compared against the phage database and each other by phylogenetics and comparative genomics. The new isolates had only three distant relatives from the database, but displayed a high overall degree of genomic similarity amongst them. The latter allowed for the use of one isolate as a representative to conduct transmission electron microscopy and structural protein sequencing, and to study phage adsorption and growth kinetics. The microscopy and proteomics tests confirmed the observed diversity of the new isolates and supported their classification to the family *Siphoviridae* and the proposal of the new phage genus “Silenusvirus”.

Lactic acid bacteria are microorganisms that can have profound value to humans. Some species protect food and feed products from spoilage bacteria via acidification and act as sensory biomodulators by fermenting different food matrices¹. Moreover, benefits of those lactic acid bacteria recognised as probiotics entail health-promoting effects². Beneficial to humans lactic acid bacteria are presently encompassed within the genera of *Lactococcus*, *Pediococcus*, *Streptococcus*, *Enterococcus*, *Oenococcus*, *Leuconostoc*, *Lactobacillus*, *Fructobacillus*, *Weissella* and *Carnobacterium*^{3–5}. A member of the genus *Lactobacillus*, *L. plantarum* is a versatile lactic acid bacterium of great potential for the food industry. This is due to the increasing popularity of *L. plantarum* as starter and adjunct culture from dairy to wine fermentations^{6,7}. Not least, many studies have suggested that supplementation with this bacterial species can have many advantages to the health and welfare of crop plants⁸. Nevertheless, the various applications of *L. plantarum* are at stake because of possible disruptions by bacteriophages (phages) infecting these bacteria, as well reported for other lactic acid bacteria^{8–10} and probiotic strains of *L. plantarum*⁵.

Effective control strategies against phages of *Lactobacillus* sp. can be facilitated with deep knowledge of their biology and genetic diversity. Unfortunately, the diversity of most reported *Lactobacillus* phages has not been thoroughly addressed¹¹. *L. plantarum* phages’ diversity, in particular, seems to be great, but has generally been grounded on morphological and growth kinetics data, and seldom on genome analyses. Based on morphological data, the capsid diameter of all known *L. plantarum* phages spans from 52 ± 2 nm (Lactobacillus phage phiLP2) to 92.7 ± 3.5 nm (Lactobacillus phage Dionysus)^{12,13} and their tail can be from 157 ± 10 nm long (Lactobacillus phage ATCC 8014-B1) to 292 ± 10 nm long (Lactobacillus phage phi14-C8)^{6,12,14}. Further, available

¹Department of Environmental Science, Aarhus University, Frederiksborgvej 399C, Roskilde, 4000, Denmark.

²Department of Clinical Microbiology, Rigshospitalet, Copenhagen, 2100, Denmark. ³Department of Plant and Environmental Sciences, University of Copenhagen, Thorvaldsensvej 40, Frederiksberg, 1871, Denmark.

⁴Department of Microbiology and Biotechnology, Max Rubner-Institut, Hermann-Weigmann-Straße 1, Kiel, 24103, Germany. ✉e-mail: lhha@plen.ku.dk

growth kinetics measurements provide a latent period between 19 min (Lactobacillus phage Y1) and 135 min (Lactobacillus phage P2)^{12,15} and a burst size between 10.8 ± 0.4 (Lactobacillus phage FAGK2) and 214.5 ± 4 (Lactobacillus phage P2)^{15,16}. At the same time, the current taxonomy of *Lactobacillus* phages has been limited to two families, *Herelleviridae* and *Siphoviridae*, although a proposal that extends it to the family *Myoviridae* has been recently published¹³. The *Herelleviridae* family hosts just two species members, *Lactobacillus virus Lb338-1* and *Lactobacillus virus LP65*, while *Siphoviridae* includes the two genera of *Lactobacillus* phages to have been officially approved by the International Committee on Taxonomy of Viruses (ICTV)¹⁷. The first genus is called “*Cequinquevirus*” and contains the species *Lactobacillus virus C5*, *Ld3*, *Ld17*, *Ld25A*, *LLKu* and *phiLdb*^{18,19}. The second genus is called “*Coetzevirus*” and involves the species *Lactobacillus virus phiJL-1*, *Pediococcus virus clP1* and *Lactobacillus virus ATCC 8014-B1*¹⁹.

Here we report the discovery of three new *Lactobacillus* phages that target industrially relevant strains of *L. plantarum*. We identify considerable genetic diversity between the newly isolated phages and the *Lactobacillus* phages of the database, which we ground on morphological, growth kinetics, as well as genomic data. Further, our results highlight the need to revisit and fully characterise prior isolates, to better appreciate the complete spectrum of diversity of *Lactobacillus* phages.

Methods

Environmental samples, phage assays and bacterial strains. *Lactobacillus* phages were isolated from organic household waste samples. The samples were collected from two different organic waste treatment plants in Denmark (treatment plants A and B). Initially, the samples were split into two subsamples and processed as detailed in Kyrkou *et al.*¹³. The resulting filtrates were screened for phages using the double agar overlay method²⁰ and a top layer of 0.4% w/v agarose. Specifically, efficiency of plating assays were performed against two indicator strains that had earlier been acquired from private collections, *L. plantarum* L1 (wine fermentation isolate) and *L. plantarum* MW-1 (grape isolate). Single plaques were resuspended in 0.7 mL SM buffer and later filtered by 0.45- μ m pore size PVDF spin filters (Ciro, Florida, USA). Each purified plaque underwent two further re-isolation-filtration cycles to ensure pure stock cultures and was stored at 4°C. For transmission electron microscopy (TEM) and protein sequencing, lysates of 10^{10} plaque-forming units (PFUs)/mL were further purified and concentrated using caesium chloride (CsCl) gradient ultracentrifugation, as described elsewhere²¹. All incubations of phage manipulations were done at 25°C using De Man, Rogosa and Sharpe (MRS) broth and agar media supplemented with 10 mM CaCl₂ (MRS), whereas indicator strains were grown in MRS at 37°C.

TEM analysis and structural protein sequencing. Phage morphology and structural proteins were determined using the CsCl-purified stocks. Micrographs of phage Silenus were generated as in other studies^{13,22}. The mean values and standard deviations of all Silenus virion dimensions were elucidated after inspection of 20–23 phage particles. Structural proteins were sequenced following published protocols^{13,22}. Briefly, 100 μ L of the CsCl-purified stocks were filtered through an Amicon Ultra filter unit (MWCO 30 kDa) and desalted four times. Phage particles (10 μ L) were denatured in 6 M urea, 5 mM dithiothreitol and 50 mM Tris-HCl (pH 8) and destabilised by freeze-thawing. Proteins were reduced (1 h incubation, 60°C) and alkylated in 100 mM iodoacetamide and 50 mM ammonium bicarbonate, digested with 0.8 μ g trypsin in 50 mM ammonia bicarbonate (40 μ L) and diluted in 0.05% trifluoroacetic acid. The resulting peptides were analysed with an Ultimate 3,000 RSLCnano UHPLC system coupled with an analytical column (75 μ m \times 250 mm, 2 μ m C18) and a Q Exactive HF mass spectrometer (ThermoFisher Scientific, Denmark). The twelve most intense ions were selected using MS Orbitrap scans and subsequently MS/MS-fragmented at a normalised collision energy (28) and a resolution of 60,000 (m/z 200). The output data were analysed in Proteome Discoverer 2.2 (ThermoFisher Scientific) and searched against predicted phage proteins by the Sequest HT algorithm.

Phage DNA isolation, library construction and sequencing. Phage DNA was extracted from the filtered stock lysates according to a standard phenol/chloroform method²³. Sequencing libraries were constructed with the Nextera[®] XT DNA kit (Illumina Inc., San Diego, California, USA) according to the manufacturer's instructions for library preparations. The library normalisation, pooling and sequencing were done as indicated elsewhere²⁴. All phage genomes were sequenced as a part of a flowcell on the Illumina MiSeq platform using the v2, 2 \times 250 cycles chemistry.

Bioinformatics analyses. *De novo* genome assembling was done with SPAdes (v. 3.5.0)²⁵ and the assemblies were cross-verified with Unicycler (v. 0.4.3)²⁶ and CLC Genomic Workbench (v. 9.5.3; CLC bio, Aarhus, Denmark) according to already published methods^{13,27}. The annotation pipeline involved automatic protein annotations with RASTik²⁸ and GeneMark²⁹ as a gene caller, followed by manual curations based on the predictions of BLASTp, HHpred³⁰ and sometimes PfamScan³¹. Lysin amino acid sequences were multiply aligned with Clustal Omega and viewed with MView (v. 1.63) using the default settings³². Transmembrane domains were identified with TMHMM³³. The genome of phage Sabazios was scanned for -1 frameshift slippery sequences near the two lysin genes with FSFinder³⁴ and all genomes were scanned for tRNA genes with tRNAscan-SE (v. 2.0)³⁵.

The analyses for the taxonomic classification of the new phage isolates followed the criteria and analyses scheme recommended by ICTV^{36,37}. For each pair of compared query-subject phage genomes, Blastn query cover was multiplied by identity, according to the crude method for estimating nucleotide similarity of ICTV³⁶. For more stringent comparisons on the nucleotide level the tool Gegenees³⁸ was used, after customising the fragment size/sliding step size (50/25) and threshold (0%). Gegenees divides a full genome (query) into fragments, then searches for BLAST “seeds” of each fragment against another genome (reference). The final phylogenomic distance of a query from a reference is the average value of all fragments' BLASTn scores expressed as a percentage of the score each fragment would yield towards itself (at 100% identity). Phylogenetic analyses were conducted

for the phages Silenus, Sabazios, Bassarid, and compared to phages that returned a Gegenees score of at least 0.05. Two phylogenetic trees were built with the default pipeline of “One Click mode” (<http://phylogeny.Lirmm.fr/>)³⁹. The first tree was based on the major capsid protein, the second on the large subunit terminase. All-against-all protein homology checks were performed between and within proteomes of the phages studied here and their closest relatives. The CMG-biotools package⁴⁰, which implements the BLASTp algorithm, was chosen for this purpose. Pairs of proteins that aligned for at least 50% of the longest sequence and shared at least 50% of their nucleotides within the aligned region were considered as positive hits. Visualisation of genome alignments among the phages of this study and their two closest phage relatives were done with Easyfig⁴¹ and the BLASTn algorithm.

Phage adsorption and growth kinetics. Phage adsorption and one-step growth experiments were done at a multiplicity of infection of 0.05. Strain MW-1 was grown to an OD₆₀₀ of 3.2, which corresponds to approximately 10⁸ colony-forming units (CFUs)/mL for this strain. Immediately after, MW-1 cultures were infected with phage Silenus and incubated for 10 min at 37 °C. This time of infection was recorded as time point zero. The remaining steps of the adsorption assay and the burst size assay followed an already published protocol²² under shaking conditions and at an incubation temperature of 37 °C. Phage growth kinetics were monitored on four-fold dilutions of the infected MW-1 cultures in triplicate assays. Samples were harvested from each triplicate assay approximately every 5–10 min, serially diluted and plated against a lawn of MW-1, incubated overnight and then examined for plaques. Supernatants of the infected MW-1 cultures just before the dilution step were plated, as well. The total count of PFUs (unadsorbed phages) from these supernatants designated how many plaques should be disregarded when counting infected centers.

Genomic data availability. Assembled and annotated genomes of phages Silenus, Bassarid and Sabazios were uploaded to GenBank under accession numbers MG765278, MG765275 and MH809528, respectively.

Results and Discussion

Phage isolation and burst size. Phages Silenus, Sabazios and Bassarid were all isolated from the organic waste samples. Phages Silenus and Sabazios came from treatment plant B and phage Bassarid from treatment plant A. The phages formed plaques of approximately 1 mm following an incubation period of 24 h at 25 °C in MRS broth and agar media (see Supplementary Fig. S1). *Lactobacillus* phage Bassarid was isolated after infecting the lawn of *L. plantarum* L1, while the other two phages were active against *L. plantarum* MW-1. Adsorption and one-step growth curve tests were performed using Silenus as the representative of the three phages, due to the overall high genomic and morphological similarities among the three phages (details in “Phage morphology”, “Support for the description of a new *Lactobacillus* phage genus” below). The adsorption rate for Silenus was 99.7%, the latent period was 45 ± 5 min and the average burst size was 4.86 progeny virions (for raw data and growth curve see Supplementary Table S1 and Supplementary Fig. S2). Although the burst size of Silenus was low, similar burst sizes have been reported for other *Lactobacillus* phages^{16,42,43}.

Phage morphology. Most virion-associated genes among phages Silenus, Sabazios and Bassarid were highly conserved (please read “Support for the description of a new *Lactobacillus* phage genus” and genomic synteny comparison results there) and their virion morphologies were similar (see Supplementary Table S2 and Fig. S3). For these reasons, phage Silenus was selected as the representative of the three phages for the morphology-related analyses. Transmission electron micrographs displayed phage particles with an isometric head (diameter: 55.6 ± 3.2 nm), a neck passage with thin whiskers, a non-contractile flexible tail (length counting including the baseplate: 173.6 ± 5.6 nm; width: 12.0 ± 0.5 nm) and a characteristic double-disc baseplate (length: 12.2 ± 1.0 nm; width: 20.2 ± 1.4 nm) which culminates in short flexible appendages with tiny terminal globular structures. Similar flexible globular structures and capsid-tail dimensions have been observed for other *Lactobacillus* phages but their exact role remains unknown^{3,12}. Interestingly, in some *Leuconostoc mesenteroides* phages similar baseplate appendages could also adsorb to other parts of the tail in an inconsistent manner⁴⁴. These characteristics classify Silenus to the order *Caudovirales* and the family *Siphoviridae* (Fig. 1), which is the most widespread taxonomic classification among *Lactobacillus* phages¹².

Basic genomic characteristics. Sequencing reads for each phage were assembled into single contigs of high coverage (667.7x–2,063x). The genome statistics of Silenus, Sabazios and Bassarid are presented in Table 1. Their genome sizes render them some of the smallest phages infecting *L. plantarum* together with phage phiJL-1 and phage ATCC 8014-B1 (accession numbers: NC_006936 and NC_019916), while their G/C content (42.5%) is close to that of their host (44.5%). In the three 37.9–38.8 kbp, double-stranded (ds) DNA phage genomes, all predicted open reading frames (ORFs) were located at the sense strand, which is in accordance with other phages of *L. plantarum*⁴⁵ and the closely-related *Pediococcus damnosus*⁴⁶. The total number of predicted ORFs was 58–62 for the three phages. Out of this total, specific functions were assigned to 18 coding sequences for phages Bassarid and Silenus and to 19 for phage Sabazios. This translated to a mean of 30.7% of their coding sequences based on the *in silico* open reading frame predictions (Table 1).

Description of phage modules. Three different genetic modules could be discerned, which enable the following: DNA packaging, morphogenesis and lysis (see Supplementary Figs. S4–S6). On the whole, such a pattern of genome organisation corresponds to most *Lactobacillus* phage isolates³. Most of the proteins that could be assigned functions to were identified in all three phages.

DNA packaging module proteins. A gene for the small subunit terminase and a gene for the large subunit terminase were recognised in all new phage genomes. Given that identifying these genes was possible, and that large subunit terminases are conserved among related phages⁴⁷, the predicted large subunit proteins were further

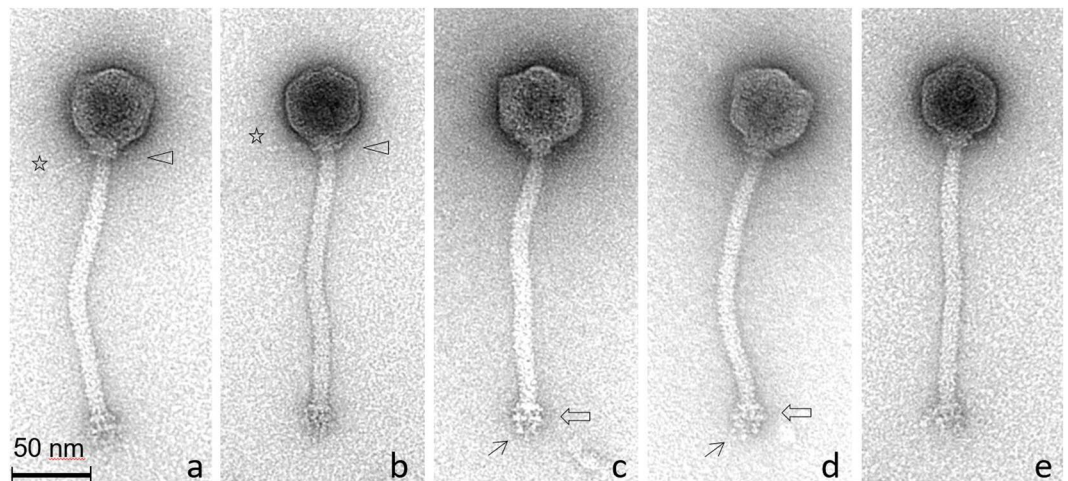


Figure 1. Transmission electron micrographs of *L. plantarum* phage Silenus. In (a, b), triangles indicate the neck passage structure with (faint) whisker structures (see stars). Open arrows in (c, d) highlight the characteristic double-disc baseplate structure at the distal end of the flexible, non-contractile tail. Single arrows in (c, d) show representative short flexible appendages (with tiny terminal globular structures) attached under the baseplate structure. The observed morphology classifies phage Silenus to the family *Siphoviridae*.

Phage Isolate	Open Reading Frames with Assigned Function/All ORFs	Genome Size (bp)	G/C Content (%)
Silenus	18/59	38,716	42.4
Sabazios	19/62	38,843	42.6
Bassarid	18/58	37,921	42.7

Table 1. Overall genome statistics of the three *Lactobacillus* phage isolates.

chosen to interrogate the phylogeny of the three phages. Downstream of the terminase unit, the sequencing coverage increased nearly twofold for all three phages. This may indicate a *pac*-type headful packaging strategy, where the variable cleaving sites for packaging termination lead to some regions being dual in some phage particles⁴⁸. A *pac*-type headful packaging was experimentally determined for the distant relatives of the three new phages, *Lactobacillus* phage ATCC 8014-B1 and *Lactobacillus* phage phiJL-1^{14,45}. For these reasons, the start of the new phages' genomes was arbitrarily set to the coding sequence of a hypothetical protein just before the small subunit terminase. The terminase unit of the new phages was located next to the morphogenesis module, as typically seen in other phages⁴⁹. In all three genomes, the portal protein constituted the junction of the DNA packaging and the morphogenesis module. Indeed, the portal protein is a crucial component of the packaging motor, because it appears to pump the phage genome into the capsid with the aid of the large subunit terminase (ATPase activity)⁵⁰. An HHpred search revealed that the extended packaging (i.e. including the portal protein) region of the three new phages was highly conserved (Fig. 5). Altogether, the interrelated *Bacillus* phages SF6 and SPP1 matched that region better than phages ATCC 8014-B1 and phiJL-1. This finding supports the *pac*-type nature of the new phages, since phages SF6 and SPP1 were shown to rely on *pac* packaging^{51,52}.

Morphogenesis module proteins. Predicted proteins of known function within the morphogenesis module of the three phages included proteins of the capsid (a scaffolding protein and a major capsid protein), proteins of the connector (the portal protein and a putative head-to-tail joining protein) and proteins of the tail (a major tail protein, a putative tape measure protein and a tail fiber protein). LC-MS/MS analysis verified that the representative phage Silenus produces two of the aforementioned proteins, one protein of the capsid (major capsid) and one of the connector (putative head-to-tail joining protein), as well as a hypothetical protein (Fig. 5; see Supplementary Table S3). The latter probably belongs to the tail, since its gene is located right downstream of the putative tape measure gene. Two more proteins have been sequenced but whether these constitute virion-associated proteins or the result of contamination is unclear (Fig. 27 and Fig. 48; Supplementary Table S3). As expected, the scaffolding protein was not traced by the protein sequencing analysis, because it comprises the core of the pre-assembled head, which is surrounded by the major capsid protein⁵³. The proteins of the capsid and the putative head-to-tail joining protein were quite conserved among the new phages and largely aligned with their orthologues in *Lactobacillus* phages ATCC 8014-B1 and phiJL-1, and *Pediococcus* phage c1P1 (BLASTp results). Similarly, the major tail and the putative tape measure proteins of Silenus, Sabazios and Bassarid contained domains with homology to the aforementioned phages and primarily to *Lactobacillus* phage phiJL-1. In the genomes of the new phages, the tape measure protein, whose length defines the length of the tail, had the longest sequence (1,066–1,078 aa) and was located downstream of the major tail protein^{54,55}. The predicted tail fiber protein of the

Bacteriophage	1	2	3	4	5	6	7	8	9	10	11
1: Lactobacillus phage phiJL-1	100.0	0.1	0.1	0.2	0.2	0.4	0.0	0.0	0.0	0.0	0.0
2: Pediococcus phage cIP1	0.0	100.0	55.1	0.0	0.1	0.1	0.0	0.0	0.0	0.0	0.0
3: Lactobacillus phage ATCC 8014-B1	0.1	55.9	100.0	0.1	0.1	0.2	0.0	0.0	0.0	0.0	0.0
4: Lactobacillus phage Silenus	0.2	0.0	0.1	100.0	63.7	29.4	0.0	0.0	0.0	0.0	0.0
5: Lactobacillus phage Sabazios	0.1	0.1	0.1	63.9	100.0	24.7	0.0	0.0	0.1	0.1	0.1
6: Lactobacillus phage Bassarid	0.4	0.2	0.2	29.9	25.4	100.0	0.0	0.0	0.0	0.0	0.0
7: Lactobacillus phage Ld17	0.0	0.0	0.0	0.0	0.0	0.0	100.0	31.7	0.0	0.0	0.0
8: Lactobacillus phage Ld25A	0.0	0.0	0.0	0.0	0.0	0.0	32.5	100.0	0.0	0.0	0.0
9: Lactobacillus phage CL2	0.0	0.0	0.0	0.0	0.0	0.0	0.0	0.0	100.0	68.7	55.4
10: Lactobacillus phage CL1	0.0	0.0	0.0	0.0	0.0	0.0	0.0	0.0	67.8	100.0	70.8
11: Lactobacillus phage iLp1308	0.0	0.0	0.0	0.0	0.1	0.0	0.0	0.0	63.3	82.4	100.0

Figure 2. BLASTn heatmap of Gegenees. Red areas illustrate phage pairs with no overall nucleotide similarity. Counterintuitive score deviations for the same pairwise comparisons, as registered on both sides of the diagonal, are due to the different lengths of compared genomes. The new phages (numbers 4–6) form a separate group.

new phages is likely to initiate the infection process through the identification and binding to host receptors on the surface of sensitive cells, as described for other phages^{56,57}. An interesting feature of the new phages' genomes was that this tail fiber protein and all hypothetical proteins found in the region between the tape measure protein and the lysis module aligned poorly with existing phage records. In average, this region exhibited low nucleotide similarity between phage Bassarid and phages Silenus, Sabazios, as well (BLASTp results; see also genomic synteny results). Considering that tail fibers shape phage host range, it is expected that the three phages' host range differs considerably from that of database phages. Moreover, tail fibers are subject to horizontal gene transfer between phages in a constant manner^{58,59}, which could explain why phage Bassarid's host range varies from that of the other two closely-related phages.

Lysis module proteins. A classic phage lysis cassette comprises two types of proteins, a holin and a lysin. Holins permeabilise the cytoplasmic membrane thereby granting access of the cell wall to lysins, which then degrade the cell wall⁶⁰. Usually, holins have two or three transmembrane domains, but the holins of the phages described in this study belonged to the rare one-transmembrane domain group⁶¹ (TMHMM search). Additionally, their best match was ORF147 from phage phiJL-1, that is likely a holin with one transmembrane domain⁴⁵. Studies indicate that *Lactobacillus* phages only employ two out of the five classes of lysins, muramidases and amidases⁶². All lysins of the phages studied here strongly matched muramidase entries (HHpred search). In this study, noteworthy was the prediction of two slightly overlapping ORFs for lysins within the module of phage Sabazios. According to Clustal Omega alignments, the first amino acid sequence of Sabazios' lysins aligned with high homology to the first 64.8% of Bassarid's and Silenus' lysin sequence. The second amino acid sequence of Sabazios' lysins aligned with a small overlap to the first amino acid sequence of Sabazios' lysins and with high homology to the last 46.5% of Bassarid's and Silenus' lysin sequence (see Supplementary Fig. S7). It is possible that these two lysins are products of a nonsense or frameshift mutation, which would create a pair of non-functional pieces⁶³. Alternatively, the two overlapping CDS may produce the subunits of a dimeric lysin, as described for phages CD27L and CTP1L of *Clostridium difficile*⁶⁴. A third scenario is that these two lysins are products of a programmed ribosomal slippage, which may either adjust the degree of lysin production as a response to conditions in the cell or produce a specific ratio of two different lysin proteins⁶⁵. So far, ribosomal slippage has principally been reported for structural genes of the tail⁶⁶. In the only studied case of slippage for *Lactobacillus* phages, both the major capsid and the major tail protein of phage A2 are affected by ribosomal slippage^{67,68}. However, FSFinder traced no slippery sequence in the overlap region of the two lysin ORFs of phage Sabazios. The fact that all predicted ORFs were found at the same strand implies the absence of genetic switches and thus, given that no other lysogeny-related genes were detected, we presume that the three new phages are most probably virulent.

Other predicted proteins. The existence of other modules could not be confirmed, but some additional proteins in the genomes of Sabazios, Silenus and Bassarid were assigned to a function. A superfamily II, ATP-dependent helicase, predicted in all three phages, may belong to the family of DEAD/DEAH-box containing helicases (BLASTp search result). DEAD/DEAH-box containing helicases participate in RNA metabolism in many, essential ways, such as by regulating gene expression and signalling⁶⁹. These functions could explain why it is likely for DEAD/DEAH-box containing helicase genes to be found within a phage genome. In all cases, the vast majority of proteins in close proximity to the new phages' helicase could not be annotated. Along with the helicase, a gene of the phages Sabazios and Silenus encoded an adenine-specific methyltransferase, which is a DNA modification enzyme. A BLASTp search revealed orthologues of Sabazios' and Silenus' methyltransferases in the genomes of *L. plantarum* and other *Lactobacillus* sp. This finding corroborates that these two phages mimic the host genome's methylation pattern as an active strategy to evade restriction by host-driven endonucleases⁷⁰. In phages, methyltransferases are often transferred through horizontal gene transfer. Genes coding for methyltransferases

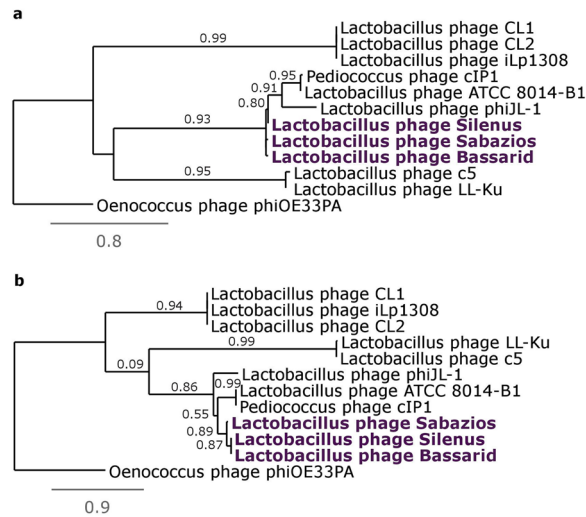


Figure 3. Phylogenetic trees constructed for phages Silenus, Bassarid, Sabazios (given in purple-coloured boldface) and those *Lactobacillus* phages that scored an average similarity of at least 0.05 or higher with Gegenees. Tree (a) was constructed using the amino acid sequences of the major capsid protein. Tree (b) was constructed using the amino acid sequences of the large subunit terminase. Comparisons were run with the “One Click mode” (<http://phylogeny.Lirmm.fr/>) and Oenococcus phage phiOE33PA proteins as an outgroup.

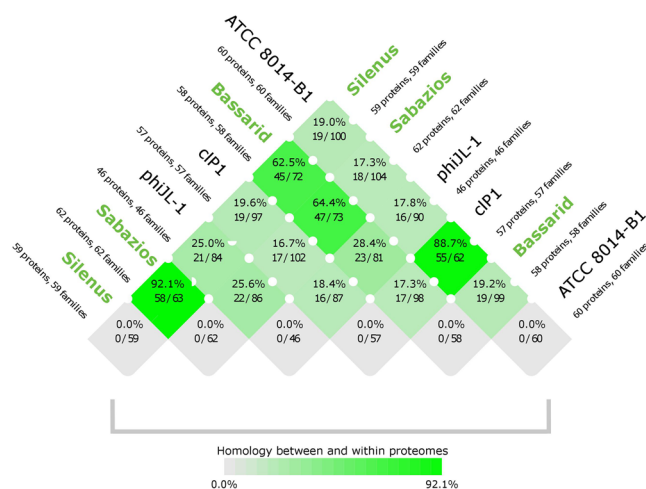


Figure 4. Homology scores of comparisons between and within proteomes. Between-proteome-comparison scores of the new phages (given in green boldface) and their closest phage relatives are in rows 1–5. Within-proteome-comparison scores (i.e. self-comparisons) are in the last row. The intense green colours signify high (>50%) proteome homology. The faded green to grey colours signify low (<50%) proteome homology. For all self-comparisons, false positive paralogue hits are avoided by skipping comparisons with an amino acid sequence against itself. In absence of paralogue hits, self-comparisons here were thus scored as 0%. The scoring was performed with CMG-biotools system.

are common in phage genomes and have already been reported in many dairy *Streptococcus* and *Lactococcus* phages^{71,72}. Methyltransferase-coding genes have also been noted in the genomes of some *L. plantarum* strains (REBASE search; <http://rebase.neb.com/rebase/rebase.html>) and in the genomes of *Lactobacillus* phages PL1 PL-1, J-1, P1174 (NCBI Protein database search).

Selfish genetic elements in the genomes of Silenus, Bassarid and Sabazios were represented by one HNH homing endonuclease. One or more HNH endonuclease genes have been found in the genomes of *Lactobacillus* phages before¹³. Essentially, HNH endonucleases are highly specialised selfish genetic elements that facilitate the mobility of themselves and of those genes to which they pertain, from genome to genome⁷³. In some cases, phages that produce HNH endonucleases can even exclude other competing phage species by cleaving their DNA⁷⁴. Due to the position of the new phages’ HNH endonuclease genes next to hypothetical genes, the role of these enzymes could not be deduced. We joined the two ORFs framing each HNH endonuclease of the studied phages and performed a BLASTn analyses. None of the resulting BLASTn hits spanned along the joint region suggesting that no gene was spliced by these HNH endonucleases.

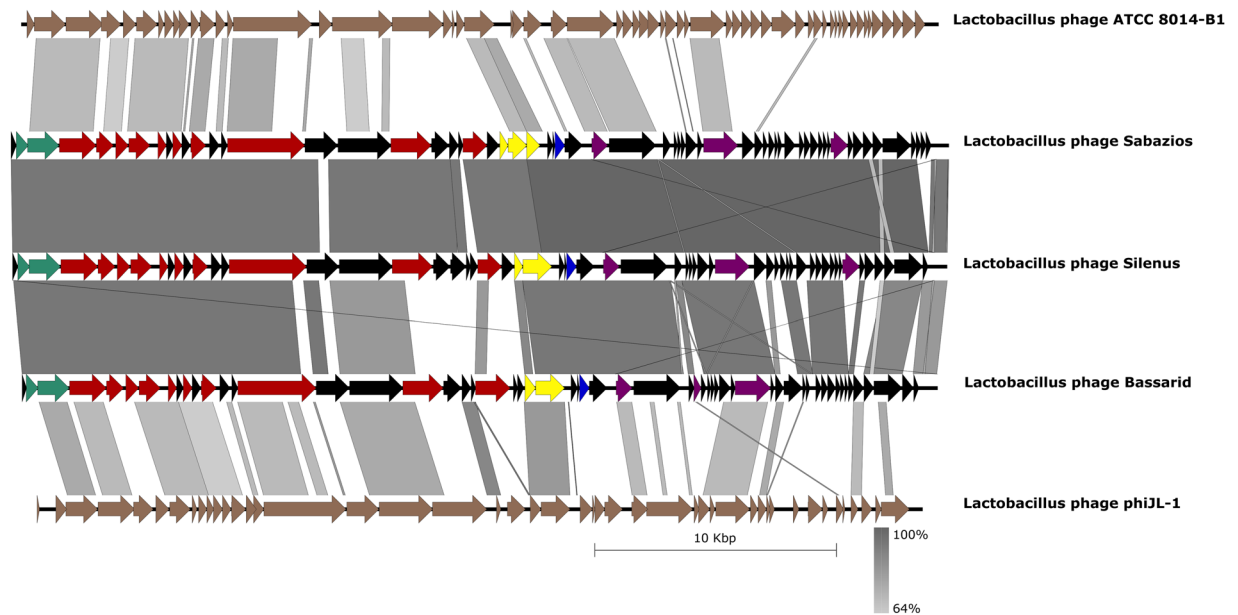


Figure 5. Genomic synteny comparisons with Easyfig and the BLASTn algorithm. The genomes of the new phages are tandemly compared to each other and to their distantly related phages ATCC 8014-B1 and phiJL-1. Arrows represent the locations of coding sequences and shaded lines reflect the degree of homology between pairs of phages. Colours other than black mark specific predicted protein functions; DNA packaging is in turquoise, morphogenesis in red, lysis in yellow, selfish genetic elements in blue and metabolism/modification of nucleic acids in deep purple.

Support for the description of a new *Lactobacillus* phage genus. Multiplying BLASTn query cover by identity yielded a limited (<50%, ICTV criterion) overall nucleotide similarity of phages Silenus, Bassarid and Sabazios to other phage records. The highest BLASTn (>50%) similarity scores were obtained from *Lactobacillus* phage phiJL-1, *Lactobacillus* phage ATCC 8014-B1 and *Pediococcus* phage cIP1. *Pediococcus* phage cIP1 has already been reported similar to *Lactobacillus* phage ATCC 8014-B1 with a high similarity score of 89%¹⁴. Such a high similarity between phages of *Pediococcus* and *Lactobacillus* is now not surprising. More and more evidence of the close phylogenetic relatedness of these bacterial genera is being gathered. Consequently, some species reclassifications between the two genera have been proposed^{75,76}. Along with these, a recent phylogenomic study examining the core- and pan-genomes of 174 type strains of *Lactobacillus* and *Pediococcus*, placed *Pediococcus* as an integral part of *Lactobacillus*⁷⁷. Phages infecting species from the one genus are thus expected to have a host range that expands to the other genus. Because *Pediococcus* and *L. plantarum* strains often coexist, the capacity of *L. plantarum* phages to infect *Pediococcus* sp. strains is indeed quite likely, as discussed for *Carnobacterium* sp. strains and other *Lactobacillus* sp. strains¹⁴. The three new phages and eight BLASTn genome records that had some level of nucleotide sequence homology to the new phages were afterwards submitted to Gegenees. All-against-all BLASTn comparisons, performed according to the Gegenees software, resulted in the heatmap of Fig. 2. The scored phylogenomic distances supported a separate grouping of the phages of this study from the other eight phages. Nonetheless, diversity within the group of the new phages was also noted, since phage Bassarid was found to be quite distinct from phages Silenus and Sabazios at the nucleotide level (average normalised similarities of 29.9% and 24.7%).

The phylogenetic trees of the major capsid protein and the large subunit terminase protein corroborated the sorting of the new phages into one individual group (Fig. 3a,b, respectively). On the other hand, diversity within the group was reiterated with phage Bassarid showing occasional, yet low variation (Fig. 3b). Consistent with earlier observations was the clustering of the three phages and phages phiJL-1, ATCC 8014-B1 and cIP1 into sister groups. Proteome homology tests were done for the new phages and those phages that appeared to be their distant relatives according to the aforementioned tests (i.e. phiJL-1, ATCC 8014-B1 and cIP1). Homology between and within the six phages further clarified how diverse these phages are from existing phage records. Specifically, the three phages share between 62.5–92.1% of their proteome (Fig. 4), while the homology to the proteomes of phiJL-1, ATCC 8014-B1 and cIP1 is low (<28.4%). Regarding homology within each phage proteome, no paralogous proteins were found for any of the six examined phages (last row of Fig. 4).

Finally, genomic synteny tests with Easyfig visualised the previously manifested homology among the new phages and provided evidence for their conserved genome architecture (Fig. 5). The major differences between phage Bassarid and the other two new phages were localised in the region of the tail-related structural genes, and particularly at those hypothetical ORFs that neighbour the tail fiber gene (see Supplementary Fig. S6). Nonetheless, no important structural dissimilarities between the tails of Silenus, Sabazios and the tail of Bassarid were further highlighted by TEM (see Supplementary Table S2 and Fig. S3). At the same time, it is seen from Fig. 5 that even if phages phiJL-1 and ATCC 8014-B1 showed some conserved gene order against the new phages

they did score low in nucleotide homology. A comparison map against phage cIP1 is available as Supplementary Fig. S8.

Taken together, all these results suggest that *Lactobacillus* phages Silenus, Bassarid and Sabazios form a coherent group and are considerably distinct from all other fully-sequenced phages. Therefore, and in agreement with ICTV criteria³⁶, we propose the new *Lactobacillus* phage genus “Silenusvirus”. At present, the new genus should consist exclusively of phages Silenus (founder), Bassarid and Sabazios.

Conclusions

A few phages of *L. plantarum* have been isolated over the years¹², but this study reports the first of these which can infect wine-related strains of *L. plantarum*. We characterised and propose three new phage species, *Lactobacillus virus Sabazios*, *Lactobacillus virus Bassarid* and *Lactobacillus virus Silenus*, by means of whole-genome sequencing and *in silico* protein prediction. Furthermore, we assessed the growth parameters of a representative phage and investigated its morphology with TEM. By comparing the phages Sabazios, Bassarid and Silenus to existing phage records, we demonstrated substantial genomic heterogeneity. This heterogeneity was further evident by the fact that we could assign functions to less than one third of the predicted ORFs. Our findings support the creation of the novel *Lactobacillus* phage genus “Silenusvirus”, with phages Silenus, Sabazios and Bassarid as the new members of this proposed genus. The results of this study shed more light on the diversity of *L. plantarum* phages and their hosts, and could aid towards the development of efficient phage control interventions in the future.

Data availability

All data generated or analysed during this study are included in this published article (and its Supplementary Information files).

Received: 23 August 2019; Accepted: 4 May 2020;

Published online: 29 May 2020

References

1. Axelsson, L. & Ahrné, S. Lactic acid bacteria. In Priest, G. F. & Goodfellow, M. (eds.) *Applied Microbial Systematics*, chap. 13, 367–388, <https://doi.org/10.1007/978-94-011-4020-1> (Springer-Verlag, Dordrecht, Netherlands, 2000), 3 edn.
2. Ljungh, A. & Wadström, T. Lactic acid bacteria as probiotics. *Curr. Issues Intest. Microbiol.* **7**, 73–90 (2006).
3. Murphy, J., Mahony, J., Fitzgerald, G. & van Sinderen, D. Bacteriophages infecting lactic acid bacteria. In McSweeney, P., Fox, P., Cotter, P., Everett, D. (eds.) *Cheese*, vol. 1, chap. 10, 249–272, <https://doi.org/10.1016/B978-0-12-417012-4.00010-7> (Academic Press, 2017), 4 edn.
4. O’Sullivan, O. *et al.* Comparative genomics of lactic acid bacteria reveals a niche-specific gene set. *BMC Microbiol.* **9**, 50, <https://doi.org/10.1186/1471-2180-9-50> (2009).
5. Endo, A. & Dicks, L. The genus *Fructobacillus*. In Holzapfel, W. & Wood, B. (eds.) *Lactic Acid Bacteria: Biodiversity and Taxonomy*, chap. 22, 381–9, <https://doi.org/10.1002/9781118655252.ch22> (John Wiley and Sons, Ltd, Chichester, England, 2014).
6. Marcó, M., Moineau, S. & Quiberoni, A. Bacteriophages and dairy fermentations. *Bacteriophage* **2**, 149–158, <https://doi.org/10.4161/bact.21868> (2012).
7. du Toit, M., Engelbrecht, L., Lerm, E. & Krieger Weber, S. *Lactobacillus*: the next generation of malolactic fermentation starter cultures—an overview. *Food Bioprocess Tech.* **4**, 876–906, <https://doi.org/10.1007/s11947-010-0448-8> (2011).
8. Lamont, J., Wilkins, O., Bywater-Ekegård, M. & Smith, D. From yogurt to yield: Potential applications of lactic acid bacteria in plant production. *Soil Biol. Biochem.* **111**, 1–9, <https://doi.org/10.1016/j.soilbio.2017.03.015> (2017).
9. Kot, W., Neve, H., Heller, K. & Vogensen, F. Bacteriophages of *Leuconostoc*, *Oenococcus*, and *Weissella*. *Front. Microbiol.* **5**, 186, <https://doi.org/10.3389/fmicb.2014.00186> (2014).
10. Deveau, H., Labrie, S., Chopin, M. & Moineau, S. Biodiversity and classification of lactococcal phages. *Appl. Environ. Microbiol.* **72**, 4338–46, <https://doi.org/10.1128/AEM.02517-05> (2006).
11. Mahony, J. & Van Sinderen, D. Current taxonomy of phages infecting lactic acid bacteria. *Front. Microbiol.* **5**, 7, <https://doi.org/10.3389/fmicb.2014.00007> (2014).
12. Villion, M. & Moineau, S. Bacteriophages of *Lactobacillus*. *Front. Biosci.* **14**, 1661–1683, <https://doi.org/10.2741/3332> (2009).
13. Kyrkou, I. *et al.* Expanding the diversity of *Myoviridae* phages infecting *Lactobacillus plantarum*—A novel lineage of *Lactobacillus* phages comprising five new members. *Viruses* **11**, 611, <https://doi.org/10.3390/v11070611> (2019).
14. Briggiler, M., Garneau, J., Tremblay, D., Quiberoni, A. & Moineau, S. Characterization of two virulent phages of *Lactobacillus plantarum*. *Appl. Environ. Microbiol.* **78**, 8719–34, <https://doi.org/10.1128/AEM.02565-12> (2012).
15. Chen, X. *et al.* Characterization and adsorption of a *Lactobacillus plantarum* virulent phage. *J. Dairy Sci.* **102**, 3879–3886, <https://doi.org/10.3168/jds.2018-16019> (2019).
16. De Antoni, G. *et al.* *Lactobacillus plantarum* bacteriophages isolated from kefir grains: phenotypic and molecular characterization. *J. Dairy Res.* **77**, 7–12, <https://doi.org/10.1017/S0022029909990203> (2010).
17. Walker, P. *et al.* Changes to virus taxonomy and the International Code of Virus Classification and Nomenclature ratified by the International Committee on Taxonomy of Viruses (2019). *Arch. Virol.* 1–13, <https://doi.org/10.1007/s00705-019-04306-w> (2019).
18. Adams, M. *et al.* Changes to taxonomy and the International Code of Virus Classification and Nomenclature ratified by the International Committee on Taxonomy of Viruses (2017). *Arch. Virol.* **162**, 2505–2538, <https://doi.org/10.1007/s00705-017-3358-5> (2017).
19. Adams, M. *et al.* Ratification vote on taxonomic proposals to the International Committee on Taxonomy of Viruses (2015). *Arch. Virol.* **160**, 1837–1850, <https://doi.org/10.1007/s00705-015-2425-z> (2015).
20. Kropinski, A., Mazzocco, A., Waddell, T., Lingohr, E. & Johnson, R. Enumeration of bacteriophages by double agar overlay plaque assay. In Clokie, M. & Kropinski, A. (eds.) *Bacteriophages: Methods and Protocols*, vol. 1, chap. 3, 69–76, https://doi.org/10.1007/978-1-60327-164-6_7 (Humana Press, Totowa, USA, 2009).
21. Sambrook, J., Fritsch, E. & Maniatis, T. *Molecular Cloning: A Laboratory Manual*. (Cold Spring Harbor Laboratory, New York, USA, 1989), 2 edn.
22. Carstens, A., Kot, W., Lametsch, R., Neve, H. & Hansen, L. Characterisation of a novel enterobacteria phage, CAjan, isolated from rat faeces. *Arch. Virol.* **161**, 2219–2226, <https://doi.org/10.1007/s00705-016-2901-0> (2016).
23. Moineau, S., Pandian, S. & Klaenhammer, T. Evolution of a lytic bacteriophage via DNA acquisition from the *Lactococcus lactis* chromosome. *Appl. Environ. Microbiol.* **60**, 1832–1841, <https://doi.org/10.1007/s00705-015-2425-z> (1994).
24. Kot, W., Vogensen, F., Sorensen, S. & Hansen, L. DPS – A rapid method for genome sequencing of DNA-containing bacteriophages directly from a single plaque. *J. Virol. Methods* **196**, 152–156, <https://doi.org/10.1016/J.JVIROMET.2013.10.040> (2014).

25. Bankevich, A. *et al.* Spades: a new genome assembly algorithm and its applications to single-cell sequencing. *J. Comput. Biol.* **19**, 455–477, <https://doi.org/10.1089/cmb.2012.0021> (2012).
26. Wick, R., Judd, L., Gorrie, C. & Holt, K. Unicycler: resolving bacterial genome assemblies from short and long sequencing reads. *PLoS Comput. Biol.* **13**, 1–22, <https://doi.org/10.1371/journal.pcbi.1005595> (2017).
27. Nielsen, T. *et al.* The first characterized phage against a member of the ecologically important sphingomonads reveals high dissimilarity against all other known phages. *Sci. Rep.* **7**, 13566, <https://doi.org/10.1038/s41598-017-13911-1> (2017).
28. Brettin, T. *et al.* RASTtk: A modular and extensible implementation of the RAST algorithm for building custom annotation pipelines and annotating batches of genomes. *Sci. Rep.* **5**, 8365, <https://doi.org/10.1038/srep08365> (2015).
29. Besemer, J. & Borodovsky, M. Genemark: web software for gene finding in prokaryotes, eukaryotes and viruses. *Nucleic Acids Res.* **33**, 451–454, <https://doi.org/10.1093/nar/gki487> (2005).
30. Söding, J., Biegert, A. & Lupas, A. The hhpred interactive server for protein homology detection and structure prediction. *Nucleic Acids Res.* **33**, 244–248, <https://doi.org/10.1093/nar/gki408> (2005).
31. Finn, R. *et al.* Pfam: the protein families database. *Nucleic Acids Res.* **42**, 222–230, <https://doi.org/10.1093/nar/gkt1223> (2014).
32. Chojnacki, S., Cowley, A., Lee, J., Foix, A. & Lopez, R. Programmatic access to bioinformatics tools from EMBL-EBI update: 2017. *Nucleic Acids Res.* **45**, 550–553, <https://doi.org/10.1093/nar/gkx273> (2017).
33. Krogh, A., Larsson, B., von Heijne, G. & Sonnhammer, E. Predicting transmembrane protein topology with a hidden markov model: application to complete genomes. *J. Mol. Biol.* **305**, 567–580, <https://doi.org/10.1006/jmbi.2000.4315> (2001).
34. Moon, S., Byun, Y., Kim, H., Jeong, S. & Han, K. Predicting genes expressed via –1 and +1 frameshifts. *Nucleic Acids Res.* **32**, 4884–92, <https://doi.org/10.1093/nar/gkh829> (2004).
35. Schattner, P., Brooks, A. & Lowe, T. The tRNAscan-SE, snoscan and snoGPS web servers for the detection of tRNAs and snoRNAs. *Nucleic Acids Res.* **33**, 686–689, <https://doi.org/10.1093/nar/gki366> (2005).
36. Tolstoy, I., Kropinski, A. & Brister, J. Bacteriophage taxonomy: an evolving discipline. In Azeredo, J. & Sillankorva, S. (eds.) *Bacteriophage Therapy*, vol. 1693, chap. 6, 57–71, 10.1007/978-1-4939-7395-8_6 (Humana Press, New York, USA, 2018), 1 edn.
37. Adriaenssens, E. & Brister, J. How to name and classify your phage: an informal guide. *Viruses* **9**, 70, <https://doi.org/10.3390/v9040070> (2017).
38. Ågren, J., Sundström, A., Häfström, T. & Segerman, B. Gegenees: fragmented alignment of multiple genomes for determining phylogenomic distances and genetic signatures unique for specified target groups. *PLoS One* **7**, 1–11, <https://doi.org/10.1371/journal.pone.0039107> (2012).
39. Dereeper, A. *et al.* Phylogeny.fr: robust phylogenetic analysis for the non-specialist. *Nucleic Acids Res.* **36**, 465–469, <https://doi.org/10.1093/nar/gkn180> (2008).
40. Vesth, T., Lagesen, K., Acar, Ö. & Ussery, D. CMG-Biotools, a free workbench for basic comparative microbial genomics. *PLoS One* **8**, e60120, <https://doi.org/10.1371/journal.pone.0060120> (2013).
41. Sullivan, M., Petty, N. & Scott, A. Easyfig: a genome comparison visualizer. *Bioinformatics* **27**, 1009–1010, <https://doi.org/10.1093/bioinformatics/btr039> (2011).
42. Foschino, R., Perrone, F. & Galli, A. Characterization of two virulent *Lactobacillus fermentum* bacteriophages isolated from sour dough. *J. Appl. Bacteriol.* **79**, 677–683, <https://doi.org/10.1111/j.1365-2672.1995.tb00954.x> (1995).
43. De Klerk, H., Coetzee, J. & Theron, J. The characterization of a series of *Lactobacillus* bacteriophages. *J. Gen. Microbiol.* **32**, 61–68, <https://doi.org/10.1099/00221287-32-1-61> (1963).
44. Ali, Y. *et al.* Classification of lytic bacteriophages attacking dairy *Leuconostoc* starter strains. *Appl. Environ. Microbiol.* **79**, 3628–3636, <https://doi.org/10.1128/AEM.00076-13> (2013).
45. Lu, Z. *et al.* Sequence analysis of the *Lactobacillus plantarum* bacteriophage FJL-1. *Gene* **348**, 45–54, <https://doi.org/10.1016/j.GENE.2004.12.052> (2005).
46. Kelly, D. *et al.* Genome sequence of the phage cP1, which infects the beer spoilage bacterium *Pediococcus damnosus*. *Gene* **504**, 53–63, <https://doi.org/10.1016/j.GENE.2012.04.085> (2012).
47. Rao, V. & Feiss, M. The bacteriophage DNA packaging motor. *Annu. Rev. Genet.* **42**, 647–81, <https://doi.org/10.1146/annurev.genet.42.110807.091545> (2008).
48. Clokie, M. & Kropinski, A. *Bacteriophages Methods and Protocols: Molecular and Applied Aspects*, vol. 2 (Humana Press, Totowa, USA, 2009).
49. Black, L. DNA packaging in dsDNA bacteriophages. *Annu. Rev. Microbiol.* **43**, 267–92, <https://doi.org/10.1146/annurev.mi.43.100189.001411> (1989).
50. Moore, S. & Prevelige, P. DNA packaging: a new class of molecular motors. *Curr. Biol.* **12**, 96–98, [https://doi.org/10.1016/S0960-9822\(02\)00670-X](https://doi.org/10.1016/S0960-9822(02)00670-X) (2002).
51. Dröge, A. & Tavares, P. Bacteriophage SPP1 DNA packaging. In Catalano, C. (ed.) *Viral Genome Packaging Machines: Genetics, Structure, and Mechanism*, chap. 6, 89–101, https://doi.org/10.1007/978-1-4614-0980-9_25 (Springer, Boston, USA, 2013).
52. Santos, M. *et al.* Genomic organization of the related *Bacillus subtilis* bacteriophages SPP1, 41c, rho 15, and SF6. *J. Virol.* **60**, 702–7, <https://doi.org/10.1099/0022-1317-65-11-2067> (1986).
53. Valpuesta, J. & Carrascosa, J. Structure of viral connectors and their function in bacteriophage assembly and DNA packaging. *Q. Rev. Biophys.* **27**, 107, <https://doi.org/10.1017/S0033583500004510> (1994).
54. Katsura, I. & Hendrix, R. Length determination in bacteriophage lambda tails. *Cell* **39**, 691–698, [https://doi.org/10.1016/0092-8674\(84\)90476-8](https://doi.org/10.1016/0092-8674(84)90476-8) (1984).
55. Pell, L., Kanelis, V., Donaldson, L., Howell, P. & Davidson, A. The phage lambda major tail protein structure reveals a common evolution for long-tailed phages and the type VI bacterial secretion system. *Proc. Natl. Acad. Sci.* **106**, 4160–5, <https://doi.org/10.1073/pnas.0900044106> (2009).
56. Le, S. *et al.* Mapping the tail fiber as the receptor binding protein responsible for differential host specificity of *Pseudomonas aeruginosa* bacteriophages PaP1 and JG004. *PLoS One* **8**, e68562, <https://doi.org/10.1371/journal.pone.0068562> (2013).
57. Steven, A. *et al.* Molecular substructure of a viral receptor-recognition protein. The gp17 tail-fiber of bacteriophage T7. *J. Mol. Biol.* **200**, 351–65, [https://doi.org/10.1016/0022-2836\(88\)90246-x](https://doi.org/10.1016/0022-2836(88)90246-x) (1988).
58. Hendrix, R., Smith, M., Burns, R., Ford, M. & Hatfull, G. Evolutionary relationships among diverse bacteriophages and prophages: all the world's a phage. *Proc. Natl. Acad. Sci.* **96**, 2192–7, <https://doi.org/10.1073/PNAS.96.5.2192> (1999).
59. Haggård-Ljungquist, E., Halling, C. & Calendar, R. DNA sequences of the tail fiber genes of bacteriophage P2: evidence for horizontal transfer of tail fiber genes among unrelated bacteriophages. *J. Bacteriol.* **174**, 1462–77, <https://doi.org/10.1128/JB.174.5.1462-1477.1992> (1992).
60. Young, R. Bacteriophage lysis: mechanism and regulation. *Microbiol. Rev.* **56**, 430–81 (1992).
61. Wang, L., Smith, D. & Young, R. Holins: the protein clocks of bacteriophage infections. *Annu. Rev. Microbiol.* **54**, 799–825, <https://doi.org/10.1146/annurev.micro.54.1.799> (2000).
62. Mahony, J. *et al.* Bacteriophage and anti-phage mechanisms in lactic acid bacteria. In Vinderola, G., Ouwehand, A., Salminen, S. & von Wright, A. (eds.) *Lactic Acid Bacteria: Microbiological and Functional Aspects*, chap. 10, 139–150, <https://doi.org/10.1201/9780429057465> (CRC Press, Florida, USA, 2019), 5 edn.
63. Cartegni, L., Chew, S. & Krainer, A. Listening to silence and understanding nonsense: exonic mutations that affect splicing. *Nat. Rev. Genet.* **3**, 285–298, <https://doi.org/10.1038/nrg775> (2002).

64. Dunne, M. *et al.* The CD27L and CTP1L endolysins targeting clostridia contain a built-in trigger and release factor. *PLoS Pathog.* **10**, e1004228, <https://doi.org/10.1371/journal.ppat.1004228> (2014).
65. Ollia, A. & Cingolani, G. A shifty stop for a hairy tail. *Mol. Microbiol.* **70**, 549–53, <https://doi.org/10.1111/j.1365-2958.2008.06434.x> (2008).
66. Xu, J., Hendrix, R. & Duda, R. Conserved translational frameshift in dsDNA bacteriophage tail assembly genes. *Mol. Cell* **16**, 11–21, <https://doi.org/10.1016/j.molcel.2004.09.006> (2004).
67. García, P., Rodríguez, I. & Suárez, J. A -1 ribosomal frameshift in the transcript that encodes the major head protein of bacteriophage A2 mediates biosynthesis of a second essential component of the capsid. *J. Bacteriol.* **186**, 1714–9, <https://doi.org/10.1128/jb.186.6.1714-1719.2004> (2004).
68. Rodríguez, I., García, P. & Suárez, J. A second case of -1 ribosomal frameshifting affecting a major virion protein of the *Lactobacillus* bacteriophage A2. *J. Bacteriol.* **187**, 8201–8204, <https://doi.org/10.1128/JB.187.23.8201-8204.2005> (2005).
69. Perc˘ ulija, V. & Ouyang, S. Diverse roles of DEAD/DEAH-Box helicases in innate immunity and diseases. In Tuteja, R. (ed.) *Helicases from All Domains of Life*, chap. 9, 141–171, <https://doi.org/10.1016/B978-0-12-814685-9.00009-9> (Academic Press, 2019), 1 edn.
70. Samson, J., Magadán, A., Sabri, M. & Moineau, S. Revenge of the phages: defeating bacterial defences. *Nat. Rev. Microbiol.* **11**, 675–687, <https://doi.org/10.1038/nrmicro3096> (2013).
71. McDonnell, B. *et al.* Global survey and genome exploration of bacteriophages infecting the lactic acid bacterium *Streptococcus thermophilus*. *Front. Microbiol.* **8**, 1754, <https://doi.org/10.3389/fmicb.2017.01754> (2017).
72. Murphy, J. *et al.* Methyltransferases acquired by lactococcal 936-type phage provide protection against restriction endonuclease activity. *BMC Genomics* **15**, 831, <https://doi.org/10.1186/1471-2164-15-831> (2014).
73. Hafez, M. & Hausner, G. Homing endonucleases: DNA scissors on a mission. *Genome* **55**, 553–569, <https://doi.org/10.1139/g2012-049> (2012).
74. Goodrich-Blair, H. & Shub, D. Beyond homing: competition between intron endonucleases confers a selective advantage on flanking genetic markers. *Cell* **84**, 211–21, [https://doi.org/10.1016/S0092-8674\(00\)80976-9](https://doi.org/10.1016/S0092-8674(00)80976-9) (1996).
75. Salvetti, E., Harris, H., Felis, G. & O’Toole, P. Comparative genomics of the genus *Lactobacillus* reveals robust phylogroups that provide the basis for reclassification. *Appl. Environ. Microbiol.* **84**, e00993–18, <https://doi.org/10.1128/AEM.00993-18> (2018).
76. Haakensen, M., Dobson, C., Hill, J. & Ziola, B. Reclassification of *Pediococcus dextrinicus* (Coster and White 1964) back 1978 (approved lists 1980) as *Lactobacillus dextrinicus* comb. nov., and emended description of the genus *Lactobacillus*. *Int. J. Syst. Evol. Microbiol.* **59**, 615–621, <https://doi.org/10.1099/ijs.0.65779-0> (2009).
77. Zheng, J., Ruan, L., Sun, M. & Gänzle, M. A genomic view of lactobacilli and pediococci demonstrates that phylogeny matches ecology and physiology. *Appl. Environ. Microbiol.* **81**, 7233–7243, <https://doi.org/10.1128/AEM.02116-15> (2015).

Acknowledgements

The authors would like to thank all collaborators of the MicroWine consortium for exchange of ideas and material. We would also like to acknowledge Angela Back from Max Rubner-Institut for technical support in the TEM analysis and the companies BioVækst (treatment plant A) and HCS (treatment plant B) for supplying the waste samples. This research was funded by the Horizon 2020 Program of the European Commission within the Marie Skłodowska-Curie Innovative Training Network “MicroWine” (grant number 643063) and the Danish Research Council for Technology and Production project “Phytoprotect” (grant number DFF – 4184-00070B).

Author contributions

I.K., A.B.C. and L.H.H. conceived the project. I.K., A.B.C., M.H. and W.K. developed the methods. I.K., A.Z. and H.N. performed the analyses. I.K., A.B.C., A.M.D., L.E.J. and H.N. conducted the experiments. I.K., A.B.C., W.K., A.Z., M.H., H.N. and C.F. validated the results. I.K. wrote the first draft and later versions of the paper. I.K., A.Z. and H.N. performed the visualisation of the results. L.E.J. and L.H.H. supervised the project. L.H.H. acquired the grants. All authors reviewed the manuscript.

Competing interests

The authors declare no competing interests.

Additional information

Supplementary Information is available for this paper at <https://doi.org/10.1038/s41598-020-65366-6>.

Correspondence and requests for materials should be addressed to L.H.H.

Reprints and permissions information is available at www.nature.com/reprints.

Publisher’s note Springer Nature remains neutral with regard to jurisdictional claims in published maps and institutional affiliations.



Open Access This article is licensed under a Creative Commons Attribution 4.0 International License, which permits use, sharing, adaptation, distribution and reproduction in any medium or format, as long as you give appropriate credit to the original author(s) and the source, provide a link to the Creative Commons license, and indicate if changes were made. The images or other third party material in this article are included in the article’s Creative Commons license, unless indicated otherwise in a credit line to the material. If material is not included in the article’s Creative Commons license and your intended use is not permitted by statutory regulation or exceeds the permitted use, you will need to obtain permission directly from the copyright holder. To view a copy of this license, visit <http://creativecommons.org/licenses/by/4.0/>.

© The Author(s) 2020